Published version: https://doi.org/10.1016/j.snb.2017.06.139

Design, Fabrication and Characterisation of Silica-Titania Thin Film coated Over Coupled Long Period Fibre Gratings: Towards Bio-Sensing Applications

Palas Biswas,*,[a] Francesco Chiavaioli,*,[b] Sunirmal Jana,[a] Nandini Basumallick,[a] Cosimo Trono,[b] Ambra Giannetti,[b] Sara Tombelli,[b] Aparajita Mallick,[a] Francesco Baldini,[b] and Somnath Bandyopadhyay[a]

[a]Central Glass and Ceramic Research Institute, CSIR-CGCRI, 196 Raja S C Mullick Road, Kolkata 700032, India

[b]Institute of Applied Physics "Nello Carrara", CNR-IFAC, Via Madonna del Piano 10, 50019 Sesto Fiorentino, Italy

Corresponding authors.

E-mail address: palas@cgcri.res.in (Palas Biswas); f.chiavaioli@ifac.cnr.it (Francesco Chiavaioli)

Keywords: long period fibre grating, over coupling, thin film overlay, sol-gel-based silica-titania thin film, bio-sensing

Abstract:

We report in this paper on the application of over coupled long period fibre gratings (OCLPFGs) to detect small changes in the surrounding refractive index (SRI). In addition, the optimization of a high RI (HRI) overlay deposited over the fibre for the adhesion of biological species is described. In this investigation, we used a sol-gel-based silica-titania thin film as HRI material deposited on the grating portion by the simple and versatile dip-coating (DC) technique. The OCLPFG-based sensor was manufactured in such way that the resonant band retains good visibility (near the maximum coupling condition) in the transmission spectrum even after high thermal sintering of the coating material. Three different batches of OCLPFGs were produced using different withdrawal speeds and sol viscosities. By carefully tuning both the overlay thickness during the DC process and the RI of the sol-gel material during its preparation, it is possible to bring the sensor in the so-called transition mode working region, and thus to maximize the sensing performance in terms of SRI changes. All the devices were characterized as optical refractometers in the RI range of interest for a bio-sensing application (from 1.33 to 1.34) and, after a suitable bio-functionalization process, one of them was used to implement a classical receptor-analyte biosensor.

Published version: https://doi.org/10.1016/j.snb.2017.06.139

1. Introduction

In recent years, long period fibre gratings (LPFGs) are becoming increasingly popular for label free bio-sensing applications [**1-7**]. The basic idea is to immobilize a selected biological species, termed as receptor, onto the fibre surface of the LPFG and hence to quantify the binding interaction with the specific analyte by measuring a signal change, i.e. the wavelength shift of the LPFG resonant band. In general, taking advantage of its resonant coupling between the fundamental core mode and the cladding modes, LPFGs are able to sense a change in the surrounding refractive index (SRI) in real time, thus representing one of the easier and most effective method for the label-free detection of target analytes, such as bio-molecules [**8**]. It was proved that conventional LPFG-based sensors, although successfully applied in this field [**3]**, need improvement in terms of RI sensitivity for a better and more accurate detection of very low concentrations of analyte: actually, when a LPFG is used for bio-sensing applications, the surrounding medium or the analyte solvent is mostly either water or a buffer solution, such as phosphate-buffered saline (PBS), having a RI close to that of water. Therefore, the method of etching or side polishing the LPFG region is not effective in this field of application because the inherent sensitivity of the resonant cladding modes around the RI of water is very low [**9**], even if higher order modes beyond $LP_{0,10}$ are considered. A sensitivity of ~1000 to ~1500 nm/RIU can be obtained using specially designed LPFG sensors with a dual-band resonance at the so-called turn-around-point (TAP) of the cladding mode [**10**]. The main issues of this kind of grating are that the bandwidth of the resonance at the TAP is larger and increases with the order of cladding mode and, when the resonance splits into two resonances beyond the TAP, the total bandwidth to monitor is huge going roughly from 1200 nm up to 1700 nm. This requires the use of broadband white light sources (e.g. a halogen lamp), which have very low power spectral density. These aspects strongly affect the measurement accuracy and resolution [**11]**. Therefore, the most interesting approach to enhance the RI sensitivity was found to be the deposition of a thin film overlay with a RI higher than that of the fibre cladding material. This allows the resonant mode of interest to operate around its transition region where, depending on the mode, on the RI of the overlay material and on its thickness, the resonance wavelength shift can be made large enough and hence a great increase in the detection sensitivity is feasible [**5**]. In this condition, the cladding modes shift their effective RI (ERI) to higher values and, when the overlay is thick enough, one of the cladding modes starts to be guided by the overlay: the mode with the highest ERI (lowest order cladding mode) becomes guided. This causes a re-organization of the ERI of all modes [**5**].

Different methods are available for the deposition of a thin film onto the LPFG surface, such as the Langmuir-Blodgett (L-B) technique, ionic self-assembled multilayer (ISAM) of thin films and electrostatic self-assembly (ESA) methods. The use of these technique is not so frequent for bio-sensing applications because of the cost involvement and their poor mechanical and thermal stability [**1**]. Moreover, it is worth mentioning the atomic layer deposition (ALD) **[12]** and radio frequency plasma-enhanced chemical vapour deposition (PECVD) **[13]** techniques as nanometre scale precision methods. In addition, the techniques of photolithographic microfabrication (i.e. wet etching, dry etching and resist-based) [**14**] surely represent other alternatives. Finally, the dip-

Published version: https://doi.org/10.1016/j.snb.2017.06.139

coating (DC) technique is another simple and versatile option since it allows depositing a thin film with just one fabrication step.

Given the intrinsic porous nature, the use of sol-gel derived coatings can improve the surface coverage for the attachment of a larger amount of molecules. For instance, silica-titania sol-gel-based materials are widely used in different applications, such as the fabrication of photonics waveguides, because of their adjustable RI (from 1.5 to 1.9) and their easy deposition on glass. The annealing post-process of these materials on glass substrates is conducted at high temperatures, ranging from 450 °C to 600 °C. The mixing ratio of titania sol with the silica sol is important because the composite material RI can be tuned by mixing the two sols at a proper ratio [**15,16**]. In addition, high temperature annealing of the sol-gel-based material, which tends to form oxides, is very compatible with glass surface. It also enables to obtain for example oxides in the form of layers, powders, monoliths or fibres. Moreover, the combination of these materials with the DC technique can provide a lot of advantages, such as simplicity, versatility and cheapness towards mass production. Therefore, this approach can be successfully applied for sensing purposes due to their properties such as transparency, porosity and high surface coverage areas.

LPFGs coated with SnO_2 sol-gel-based materials were firstly used for gas sensing because of the sol-gel porosity, which allows gas to penetrate inside the sol-gel material and thus to change the optical characteristics in terms of optical power or wavelength [**17**]. SRI sensitivity of roughly 1067 nm/RIU in the range of 1.42-1.44 has just been experimentally shown based on silica (SiO_2, RI ~ 1.42 to 1.43) and titania (TiO_2, RI ~ 1.91 to 1.96) sol-gel-based materials [**18**] without tuning the film thickness to get it at the transition point of the cladding modes. A novel scheme of high-sensitivity relative humidity (RH) sensor based on cascaded chirped LPFG and sol-gel derived TiO_2/SnO_2 composite films has been demonstrated with a wavelength shift of 12.37 nm for RH varying from 40% to 95% [**19**]. A TiO_2-based nanoparticles thin film was also deposited over an optical fibre to make a Fabry-Perot sensor and it was shown that the developed sensor can be used as an optical refractometer by monitoring the shift of the interference fringes in the reflection spectrum [**20**]. They achieved a SRI sensitivity of 69.38 dB/RIU over the RI range 1.333-1.457. Finally, a fibre-optic pH sensor was also demonstrated using sol-gel-derived TiO_2 film doped with organic dyes **[21]**.

Here, we discuss in detail the use of the silica-titania sol-gel-derived materials as HRI (1.680-1.700) overlay deposited on the fibre surface by the DC process. For this purpose, over coupled LPFGs (OCLPFGs) as sensing devices were used instead of standard gratings. The film thickness is optimized to allow the OCLPFGs to work in modal transition when the surrounding environment is a biological solution (RI ~1.334). After the thin film deposition over fibre portion containing the OCLPFG, the sensor was annealed at high temperature (~450 °C) to sinter the mixed sol and also to bring the OCLPFG at the maximum coupling condition with enhanced transmission contrast. Three different batches of OCLPFGs have been produced using different withdrawal speeds for the optimization of the coating thickness and to compare their sensitivity in terms of volume SRI changes (nm/RIU). With one sample, a sensitivity approaching 7000 nm/RIU has been

Published version: https://doi.org/10.1016/j.snb.2017.06.139

attained considering the LP_{07} cladding mode within its modal transition region. The same sensor has also been used to implement a classical receptor-analyte (IgG/anti-IgG) assay by properly functionalising the fibre surface. The proposed HRI sol-gel coated OCLPFG-based device can be used as a feasible and effective biosensor.

2. Background Theory and Simulations

Coupled mode theory offers a practical and simple way of predicting and understanding how an LPFG behaves [**22**]. Using this approach, the wavelength of the attenuation peaks (i.e. the (resonance wavelength) present in the transmission spectrum of an LPFG can be calculated considering the phase matching condition of the modes **[22]**

$$\lambda_{res} = \left(n_{core}^{eff} - n_{clad,m}^{eff}\right)\Lambda \quad (1),$$

where λ_{res} is the resonance wavelength, Λ is the grating period, and n_{core}^{eff} and $n_{clad,m}^{eff}$ are the ERIs of the fundamental core mode and the *m*-th cladding mode, respectively. While n_{core}^{eff} is independent of the SRI (or n_{sur}), $n_{clad,m}^{eff}$ strongly depends on it since the light travelling in the fibre core does not directly interact with the surrounding medium and only the field of cladding modes extends out to the surroundings. Therefore, the change in the SRI will affect the cladding mode ERI and hence λ_{res}. The higher order cladding modes show higher SRI sensitivity than lower order ones since their fields extend mostly to the surroundings (larger penetration depth of the evanescent wave) **[8]**. In general, the λ_{res} of the cladding mode shifts towards shorter wavelengths (blue shift) when the SRI goes from air to the RI of fibre cladding; conversely, the λ_{res} shifts towards longer wavelengths (red shift) when the SRI is greater than the fibre cladding RI (> 1.45) **[9]**.

As touched in the Introduction, when an overlay with a RI greater than that of the fibre cladding is deposited over the fibre, there are important variations on the resonance condition of eq. (1), which lead to dramatic shifts of the λ_{res} if the coating is thick enough to bring one cladding mode to the guidance condition within the overlay **[5]**. In order to increase the SRI sensitivity of a particular cladding mode for a specific application, the RI and thickness of the overlay material should carefully be chosen. In fact, the λ_{res} shift is maximum when the ERI of the mode is half of its original value and the original ERI of the next lower cladding mode before the film deposition. This condition defines the optimum overlay thickness (OOT) to bring any cladding mode in its modal transition region. The value of the OOT depends not only on the previous parameters, but also on the SRI in which the measurement is carried out. In a general design rule, the first selection concerns the overlay RI considering the air as SRI. This allows to define the amount of material that is necessary to deposit and the device sensitivity. If the SRI is water, then the thickness of the overlay material has to be changed to reach the OOT in order to reach the highest sensitivity region.

Published version: https://doi.org/10.1016/j.snb.2017.06.139

By using the well-known transfer matrix method, it is possible to evaluate the OOT for different SRIs, such as air or solutions normally used in bioassay experiments, like PBS (RI = 1.334). The ERI of the selected cladding mode (in this case LP_{07}) shifts to the lower order cladding mode (LP_{06}), when the overlay thickness increases. As shown in **Fig. 1**, the LP_{07} mode will be within its modal transition region for a thickness of 350 nm when the SRI is air (RI = 1.000) and the overlay RI is 1.6 (black squares). At that thickness, the mode will nearly overlap with the lower order mode when the SRI is PBS, which is not the desirable working condition around the transition point as shown in **Fig.1**. The same phenomenon can be observed for different overlay RIs: 1.6 (squares), 1.68 (triangles) and 1.8 (stars). **Fig.1** also shows that a higher overlay RI requires a lower value of the film thickness to reach the mode transition condition when the SRI is PBS. Therefore, the second and final design rule clearly states that, when the overlay RI and the working SRI are chosen, the overlay thickness plays the crucial role.

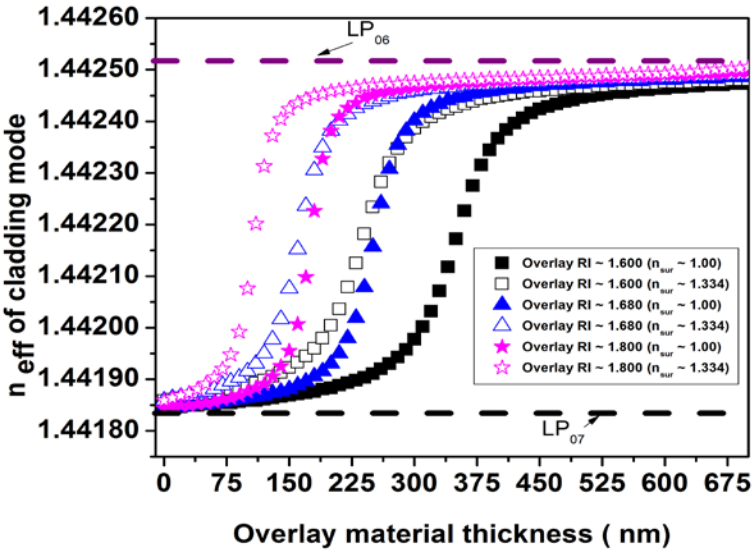

Fig. 1. Calculation of LP_{07} ERI with the increase of overlay thickness for difference RIs (1.600, 1.680 and 1.800) when the surrounding RI is air (n_{sur}~1.000) or PBS (n_{sur}~1.334) mimicked the biological environment.

3. OCLPFG fabrication

In general, standard LPFGs can be fabricated using two different inscription techniques, such as amplitude mask or point-by-point, with the help of different sources, such as CO_2 lasers, femtosecond lasers or UV lasers. With the first inscription technique, the grating length L is fixed and the condition of under or over coupling for a particular mode can be tailored by adjusting the cumulative UV exposure, which implies adjusting the RI modulation (Δn) in the fibre core that modifies the coupling coefficient (κ). The second approach allows a wider customization of the grating parameters. Therefore, LPFGs were fabricated using the second writing technique with an UV KrF pulsed excimer laser (BraggStar 500, TUI laser, Germany) working at 248 nm. LPFGs

Published version: https://doi.org/10.1016/j.snb.2017.06.139

were inscribed in a hydrogen loaded (1500 psi for 24 h at 100 °C) standard SMF28e fibre (Corning Inc., USA) with Λ equal to 340 μm.

Fig.2 sketches the power transfer between core and cladding modes of a standard LPFG as a function of the coupling constant κ·L. It is worth reminding that the maximum coupling condition in standard LPFGs states $\kappa \cdot L \cong \pi/2$ (B point). However, in order to fabricate OCLPFGs with a grating length of about 35 mm, the UV fluence was adjusted in such a way that the LP_{07} cladding mode could be over coupled ($\kappa \cdot L \gg \pi$) and the coupling constant κ·L was pushed within 5π/4 (between C and D points). This special type of strongly OCLPFGs found significant application in SRI sensors, especially where the SRI is greater than the fibre cladding RI [**23,24**]. Another advantage is that UV induced OCLPFGs can also be used after high temperature annealing processes up to 500 °C – 600 °C, that normally make unusable standard LPGs, by optimizing the initial over-coupling in order to have the maximum coupling strength after the annealing. In fact, if the initial coupling strength is in between π and 5π/4, after the high temperature annealing process, a good coupling strength of roughly 15-20 dB (resonance transmission loss) can be obtained, which is surely an important parameter in RI-based sensing applications as a narrower and deeper bandwidth of the resonance implies a lower standard deviation associated to the detection of the resonance wavelength **[8,10]**.

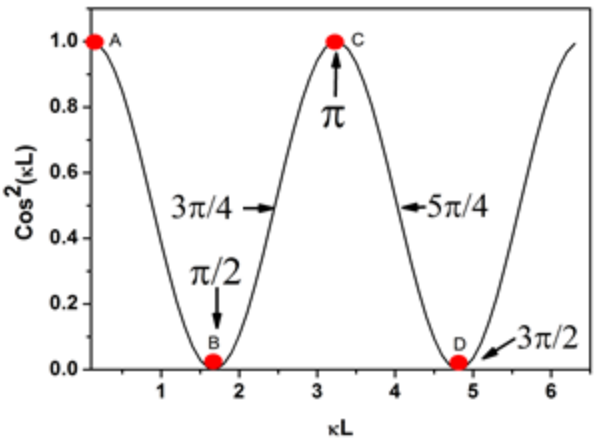

Fig. 2. Power transfer between the core and any cladding mode in LPFGs as a function of coupling constant κ·L.

As an example, **Fig.3** details the spectrum of an OCLPFG after its fabrication where LP_{07} is placed at ~1700 nm, outside the wavelength range (cyan curve). For a strongly over coupled condition, the lower order modes, LP_{02} and LP_{03}, show good attenuation strengths of about ~7.5 dB and ~11 dB, respectively. This amount of strength for lower order modes could not easily able to be obtained in standard fabricated LPFGs where $\kappa \cdot L \sim \pi/2$ (maximum coupling condition). Strongly OCLPFGs were then annealed at 550 °C for 2.5 hours. The reasons for this are essentially two: first, the grating stabilisation so that it can be safely used for the sol-gel coating that requires the grating to be heated at around 450 °C for the sol sintering; second, the reduction of the UV induced

Published version: https://doi.org/10.1016/j.snb.2017.06.139

Δn by thermal treatment so that κ·L for $LP_{0,7}$ cladding mode can be brought near π/2 to get the maximum visibility of the resonance in the transmission spectrum at the end of the fabrication process, as shown in **Fig. 3** looking at the resonance evolution (from the blue curve up to the black one).

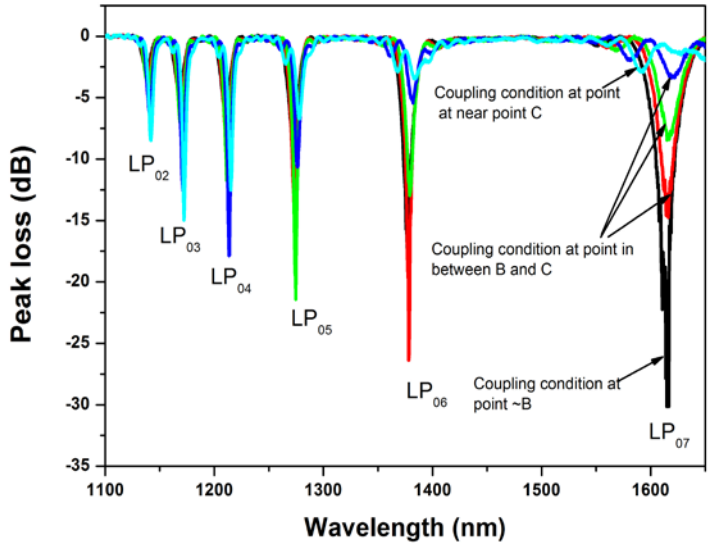

Fig. 3. Grating spectra during the fabrication steps at different over coupled conditions corresponding to the points of Figure 2. The evolution of the resonance of interest at longer wavelengths (LP_{07} cladding mode) is clearly detailed.

Three different batches of OCLPFGs have been produced using different withdrawal speeds (details in the next Section) during the deposition of the sol-gel overlay by DC for the optimization of the coating thickness. λ_{res} and transmission loss of the previous grouped OCLPFGs are shown in **Fig. 4** (after annealed in red dashed curves, before annealing in black curves) with the peaks at longer wavelengths corresponding to the LP_{07} cladding mode. **Fig. 4a, 4b and 4c** belong to the OCLPFGs of the first (OCLPFG-1), second (OCLPFG-2) and third (OCLPFG-3) batches, respectively. **Table 1** collects the measured values of λ_{res} and transmission loss (dB) for both the LP_{06} and LP_{07} modes considering all the three batches.

Published version: https://doi.org/10.1016/j.snb.2017.06.139

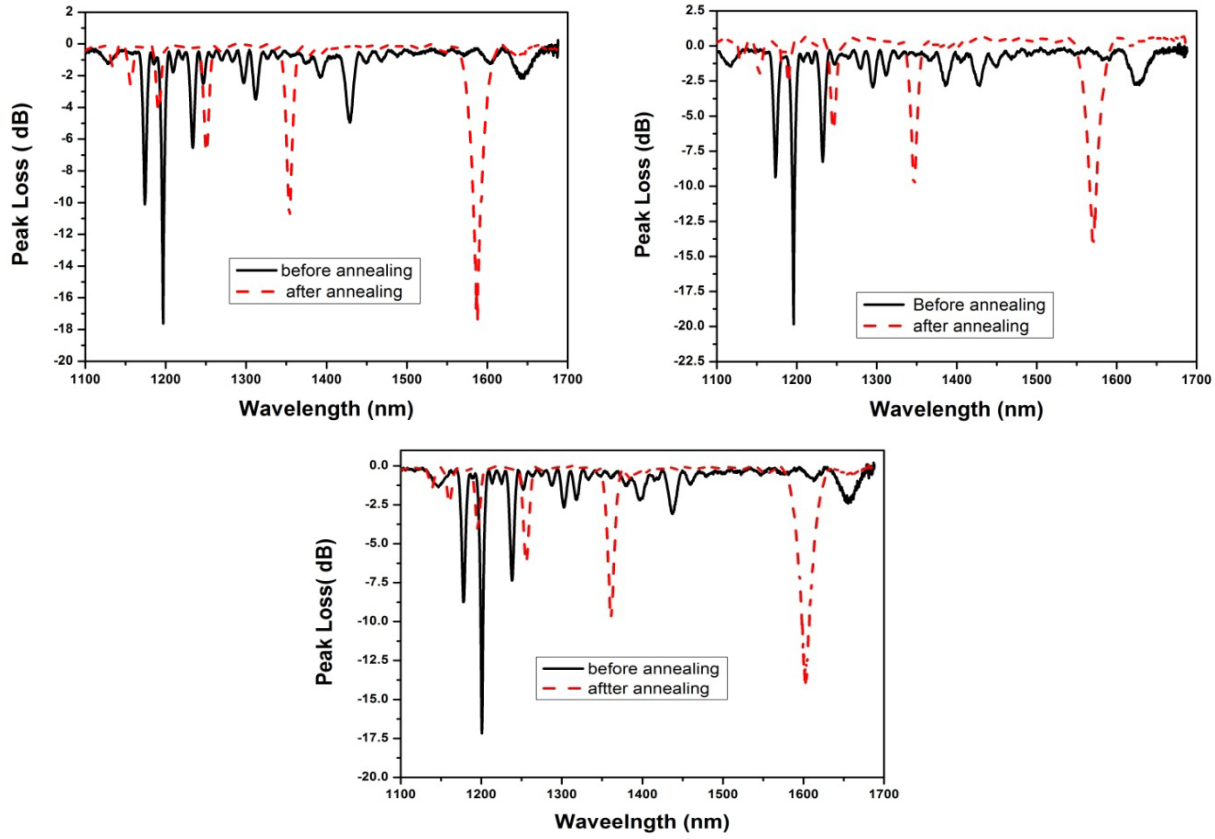

Fig. 4. Measured spectra of an OCLPFG sample from batch 1 (**a**), of an OCLPFG sample from batch 2 (**b**) and of an OCLPFG sample from batch 3 (**c**), before (black curve) and after (red dashed curve) the high temperature annealing process.

Table 1. Resonance wavelengths of LP_{06} and LP_{07} cladding modes of three different OCLPFG samples after the annealing process evaluated from the spectra of Figure 4.

Sensor ID	LP_{06}		LP_{07}	
	λ_{res} (nm)	Transmission loss (dB)	λ_{res} (nm)	Transmission loss (dB)
OCLPFG-1	1352.57	-10.6	1584.71	-16.59
OCLPFG-2	1346.15	-10.8	1571.16	-15.59
OCLPFG-3	1360.94	-9.3	1603.59	-13.5

4. Sol-gel preparation, film deposition and characterisation

Thin film deposition by sol-gel process is well known and this process was also illustrated in a previous work [**25**]. All the chemicals and reagents along with the deposition of the silica-titania sol-gel-derived film overlay were described in detail in our previous work [**26**]. However, the titania/silica ratio of sols and the RI of the final sol-gel material are 50%:50% (w/w) and 1.698,

Published version: https://doi.org/10.1016/j.snb.2017.06.139

respectively. To improve the sensor performance and to reach the OOT, the film thickness was tailored by changing the precursor sol viscosity as well as the withdrawal speed (OCLPFG-1: 2.2 mm sec^{-1}; OCLPFG-2: 2.5 mm sec^{-1}; OCLPFG-3: 2.8 mm sec^{-1}) during the film deposition. It is noted that a single deposition step was found to be sufficient to move the selected cladding mode into the modal transition region **[5,18]**. The picture in **Fig. 5a** shows both a vial containing the prepared precursor sol (on the left) and a special aluminium fibre holder with grooves for keeping straight the OCLPFG samples during the annealing process (on the right). As can be seen from **Fig. 5a**, it is possible to perform the annealing process with several fibre samples in parallel since the holder consists of a few grooves. The DC machine (Model n. HO-TH-01, Holmarc, India) used for the deposition of the film overlay is depicted in **Fig. 5b**. The control panel on the right allows customizing the parameters of the DC process.

Fig. 5. Picture of the precursor sol (sol-gel material) and the fibre holder (**a**) used during the annealing process and of the dip coating machine used to deposit the film overlay onto the OCLPFG surfaces (**b**).

The OCLPFGs fixed within the previously mentioned holder were heated in a furnace (MTI furnace, USA) to transform gel into oxide film. During the heat treatment, the temperature of the furnace was increased from 26 °C to 450 °C at a rate of about 1.2 °C min^{-1}; afterwards, the samples

Published version: https://doi.org/10.1016/j.snb.2017.06.139

were kept at 450 °C for about 2.5 h. Later, the furnace temperature was slowly cooled down with the same rate to avoid any cracks due to thermal shock.

As an example, **Fig. 6** accounts for the measured spectra in air before (black curves) and after (red dashed curves) the deposition of the sol-gel-derived film overlay. Again, **Fig. 6a, 6b and 6c** belong to the OCLPFGs of the first (OCLPFG-1), second (OCLPFG-2) and third (OCLPFG-3) batches, respectively. **Table 2** reports on the measured values of the λ_{res} shift before and after the DC process for both LP_{06} and LP_{07}. As discussed in Section 2, the value of both the λ_{res} is important to bring the considered cladding mode in its modal transition region.

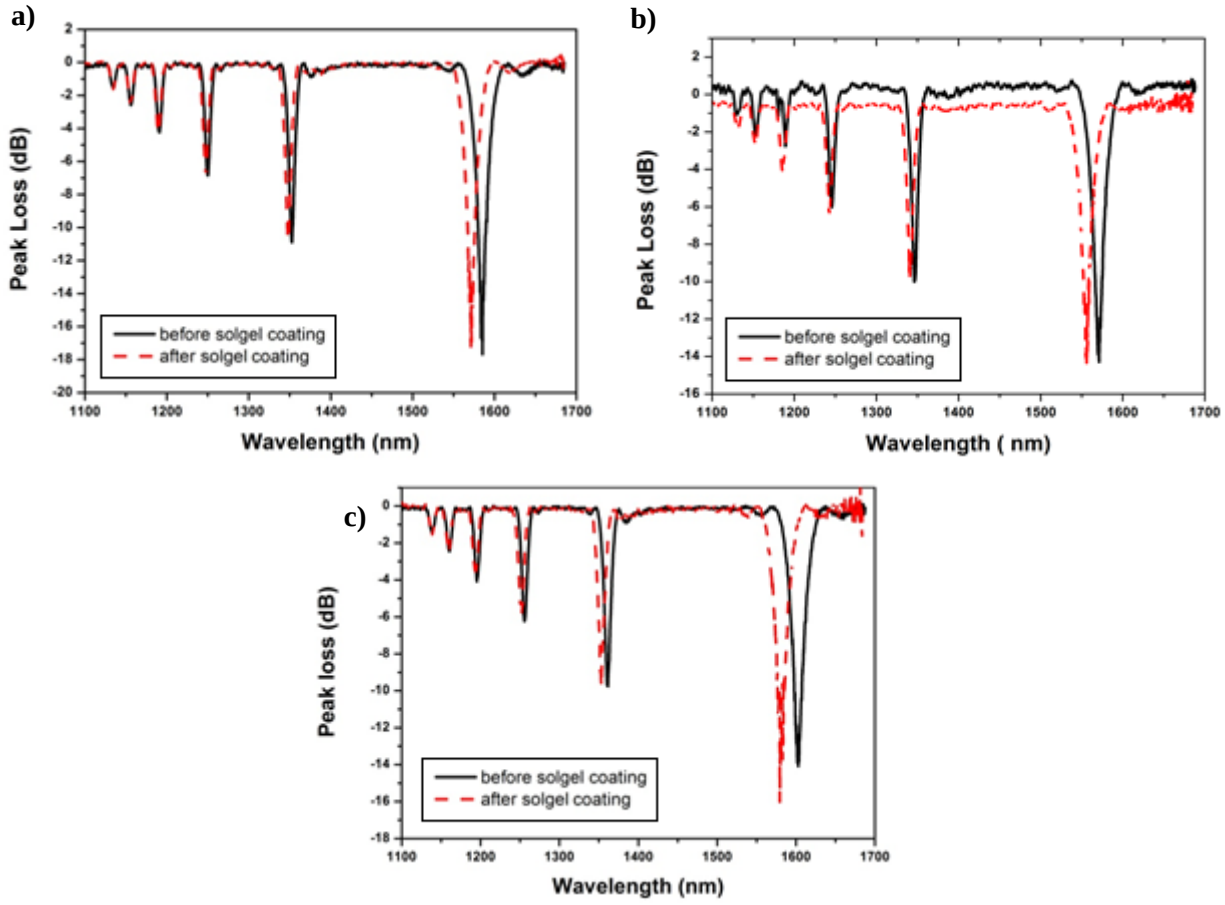

Fig. 6. Measured spectra in air before (black curves) and after (red dashed curves) the deposition of the sol-gel-derived film overlay related to an OCLPFG sample from batch 1 (**a**), to an OCLPFG sample from batch 2 (**b**) and to an OCLPFG sample from batch 3 (**c**).

Table 2. Resonance wavelength shift measured in air and evaluated from the spectra of Figure 6 before and after the deposition of the silica-titania sol-gel-derived film overlay for both LP_{06} and LP_{07} modes considering the three different OCLPFG samples.

		LP_{06}	LP_{07}

Published version: https://doi.org/10.1016/j.snb.2017.06.139

Sensor ID	Withdrawal speed (mm/sec)	λ_{res} (nm) before coating	λ_{res} (nm) after coating	λ_{res} shift (nm) in air, blue shift	λ_{res} (nm) before coating	λ_{res} (nm) after coating	λ_{res} shift (nm) in air, blue shift
OCLPFG-1	2.2	1352.57	1349.42	~ 3.1	1584.71	1571.18	~13.7
OCLPFG-2	2.5	1346.15	1340.88	~ 5.3	1571.16	1554.164	~16.8
OCLPFG-3	2.8	1360.94	1351.52	~ 9.4	1603.59	1582.59	~21.0

5. Sensitivities characterisation and analysis

5. 1 Temperature sensitivity

A standard LPFG is more sensitive to temperature changes than a fibre Bragg grating because the shift of the λ_{res} due to temperature changes depends on the difference of ERIs of core mode and cladding modes (i.e. the thermo-optic coefficient) **[9]**. The resonance wavelength can shift towards longer (red shift) or shorter (blue shift) wavelengths depending on the doping materials and the concentration of those doping materials in the fibre core during its fabrication. For instance, LPFGs fabricated in a germanium-doped silica fibre shows a red shift with the temperature increase, whereas LPFGs fabricated in a germanium-boron co-doped silica fibre exhibits a blue shift. The temperature sensitivity coefficient of the realized OCLPFGs with and without the sol-gel overlay was achieved with the help of a thermo-electric cooler (TEC) controller-based system and a Peltier cell. The fibre samples were placed in contact with a stainless steel plate (SS-316), which in turn was placed on the Peltier cell. The temperature was changed from 20.4 °C to 27.4 °C with steps of 1 °C through the controller unit. **Fig. 7** shows the evaluated temperature sensitivity of both the sol-gel coated (red line) and not coated (black line) OCLPFGs considering the same cladding mode LP_{07}. The coated sensor shows a slightly higher temperature sensitivity (~77.5 pm $°C^{-1}$) than the not coated one (~61.9 pm $°C^{-1}$) because the n_{clad}^{eff} and the thermo-optic coefficient are slightly changed due to the presence of the sol-gel overlay. The same experiment was carried out with samples of the three batches showing comparable results within 1% of error (data not showed).

Published version: https://doi.org/10.1016/j.snb.2017.06.139

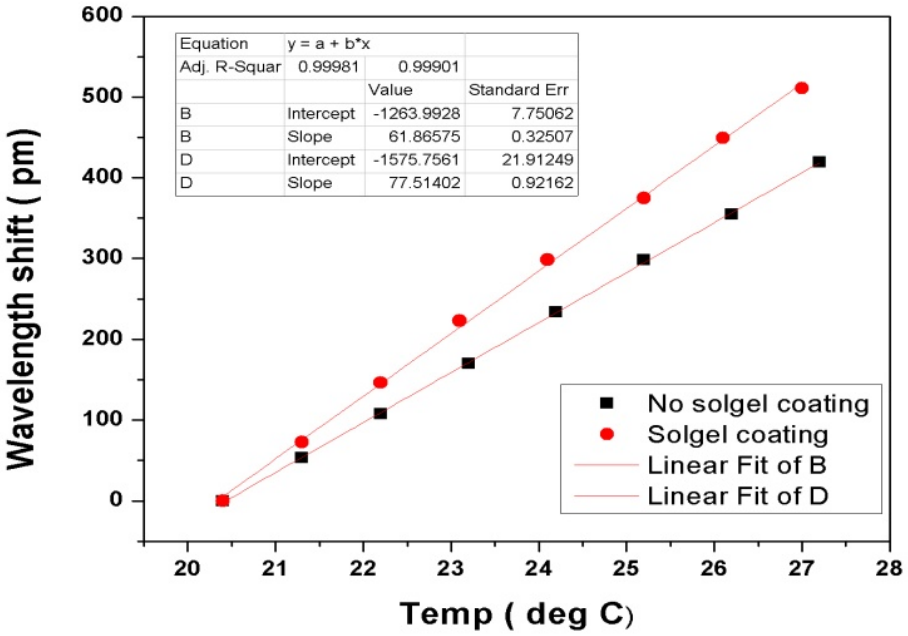

Fig. 7. Temperature sensitivity characterisation of sol-gel coated (red) and not coated (black) OCLPFGs for LP_{07} mode.

5.2 Volume SRI sensitivity

The LPFG sensitivity to SRI changes is due to the interaction of the evanescent wave, which extends out of the fibre surfaces only hundreds of nanometres (100-500 nm), with the surrounding medium. For this reason, the response of a LPFG sensor to a volume RI variation (i.e. RI change of the solution surrounding the fibre), is different from the response to a bio-molecular interaction immobilized onto the fibre surface **[8]**. However, a volume RI sensitivity test using NaCl solutions at increasing concentrations from wt. 0% (deionized water, 1.333 RIU) up to wt. 0.6% (1.3341 RIU) with step of 0.1% wt. was performed to investigate the complete behaviour of the sensors. The temperature of the experimental micro fluidic system that contains the sample in a straight condition (no bending or axial strain occur during the measurements) was fixed at 23 °C. A sample from the second batch (OCLPFG-2) was chosen for this experiment and a SRI sensitivity of roughly 7075 nm RIU^{-1} was obtained. **Fig. 8a** and **8b** show the spectral evolution and the related linear response curve for different wt. percentage of NaCl solutions, respectively. It is worth noticing that the standard deviation of the experimental points (~15 pm) of **Fig. 8b** is smaller than the symbols' dimension.

a) **b)**

Published version: https://doi.org/10.1016/j.snb.2017.06.139

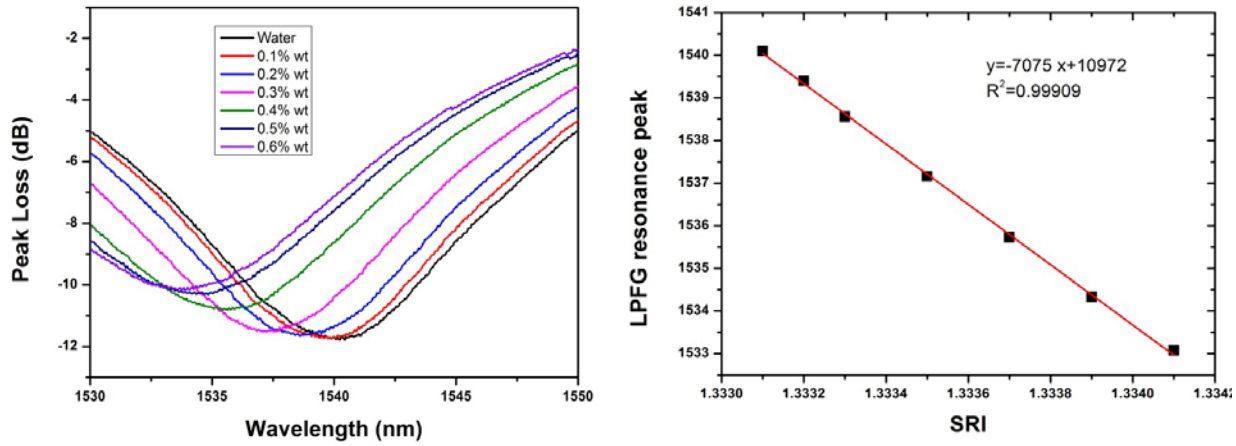

Fig. 8. Measured spectra of sol-gel coated OCLPFG from batch 2 during the SRI sensitivity test using different NaCl solutions (**a**). Response curve (λ_{res} vs. SRI) of same sample with the linear fitting curve and the obtained SRI sensitivity (**b**).

6. Thickness and RI optimization of silica-titania sol–gel thin film

As discussed in the Introduction, the SRI sensitivity of LPFGs can significantly be enhanced when the sensor works in the modal transition region. The behaviour of the LP_{07} cladding mode as a function of the thickness of the sol-gel film overlay was calculated considering an overlay RI of 1.698 RIU and the PBS buffer solution (1.334 RIU) as surrounding medium. The simulated curve (black) shown in **Fig. 9** demonstrates that the sensors can work around the most sensitive linear region within B1 and B2 points when the overlay thickness is comprised between 140 nm to 175 nm. In this way, the LP_{07} mode will be in the modal transition region when the surrounding medium is PBS and the sensor will show the higher SRI sensitivity when the biochemical interaction between the target analyte and the sensing layer takes place.

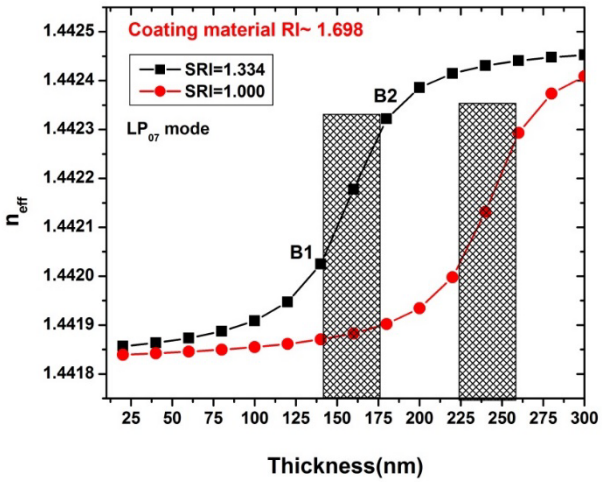

Fig. 9. n_{clad}^{eff} vs. overlay thickness simulated curves for the LP_{07} cladding mode when an OCLPFG is coated with the sol-gel material within two SRIs and considering an overlay RI of 1.698: air (red curve) and PBS (black curve).

Published version: https://doi.org/10.1016/j.snb.2017.06.139

Based on these simulations following the general approach described in **[27]**, the thickness of the silica-titania sol-gel-based film overlay was optimized by varying the viscosity of the sol and the withdrawal speed during the film deposition. However, from a practical point of view, the overlay RI can slightly vary from the desired value depending on the sol composition, on the ageing time of sol that can directly influence the sol viscosity and on the curing temperature **[14,15,25]**. In order to evaluate the sensor dependence on this parameter, the ERI of LP_{07} mode was simulated as a function of the overlay thickness, considering a ±1% change in the overlay RI (from 1.681 up to 1.714) and considering PBS as surrounding medium. The results are presented in **Fig. 10**. The ±1% variation on the overlay RI changes just slightly the sensitivity without shifting too much the sensor from the most sensitive region. Considering this variation, a tolerance on the overlay thickness of about 25 nm can be predicted. Since the DC technique cannot be considered a nanometre scale precision method like others, this value of tolerance allows keeping the sensors within the most sensitive modal transition region.

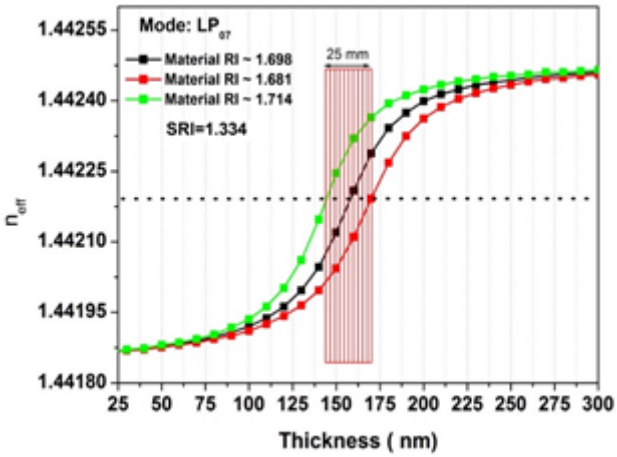

Fig. 10. n_{clad}^{eff} vs. overlay thickness simulated curves used for studying the influence of a change of 1% in the overlay RI considering the LP_{07} cladding mode when the surrounding medium is a PBS solution (SRI = 1.334) mimicked the biological environment.

Finally, the thickness of film overlay, which plays the crucial role in the SRI sensitivity optimization, was analysed by means of a field emission scanning electron microscope (FESEM, Supra 35VP, Carl Zeiss). **Fig. 11a** shows an image of the cross-section of an OCLPFG coated with the silica-titania sol-gel film overlay (the shiny white ring surrounding the fibre) considering a sample from the second batch (OCLPFG-2). The averaged thickness of the deposited film overlay was measured in different portions (**Fig. 11b**) and was estimated to be roughly 159 nm, exactly in the middle of the most sensitive modal transition region (black curves of Figures **9** and **10**). In **Fig. 11b**, the red triangle indicates the silica optical fibre (darker region), whereas the blue one specifies the silica-titania sol-gel film overlay (lighter region).

Published version: https://doi.org/10.1016/j.snb.2017.06.139

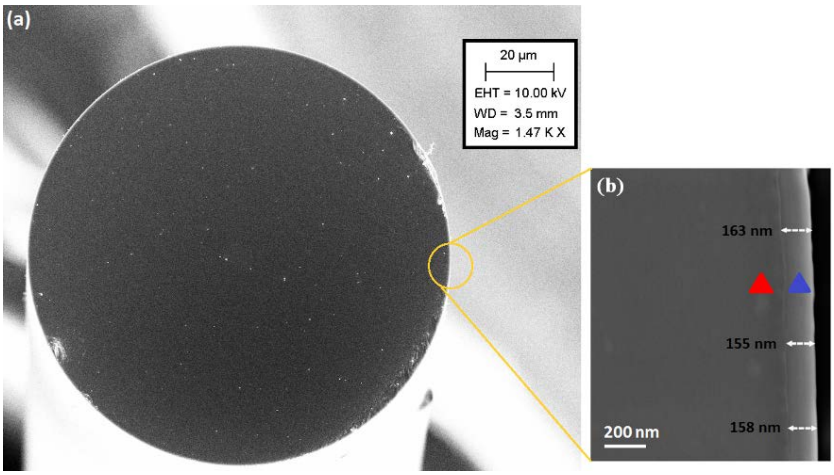

Fig. 11. FESEM image of the cross-section of an OCLPFG coated with sol-gel-based silica-titania film overlay (**a**). The image refers to a sample from the second batch. A part of the sample border highlighted in orange was enlarged to show the film overlay and its thickness measured in three different portions giving an averaged value of 159 nm (**b**).

7. Bio-sensing by using silica-titania sol-gel coated OCLPFGs

The step-by-step protocol followed to implement a classical receptor-analyte bioassay is described in [**3**]. The functionalization of the fibre surface in correspondence of the coated region was achieved by the deposition of a layer of a methacrylic acid/methacrylate copolymer (Eudragit L100) useful for antibody (receptor) immobilization. Once the fibre surface was functionalised, the sensor was placed inside a temperature-stabilised flow cell deeply described in [**28**]. All the steps for the implementation of the bioassay were carried out using the flow cell connected to a peristaltic pump and keeping the temperature of the flow cell at 23 °C. Briefly, we firstly activated the surface functionalities (–COOH carboxylic groups) by a classical cross-linking chemistry (1-Ethyl-3-[3-dimethylaminopropyl] carbodiimide hydrochloride, EDC, and N-hydroxysuccinimide, NHS), then we covalently immobilised the receptor (mouse IgG, 1000 mg L^{-1} in PBS). A washing step with PBS was done to remove the un-reacted receptors and then, the surface passivation with bovine serum albumin (BSA, 3% in PBS) was performed to block the remaining activated functionalities and thus to prevent non-specific adsorption. The assay was finalised with increasing concentrations of analyte (goat anti-mouse IgG) spiked in PBS buffer and ranging from 100 µg L^{-1} up to 100 mg L^{-1}.

The performance of the proposed biosensor was evaluated by monitoring in real time the evolution of λ_{res} during the injection of different concentrations of analyte (**Fig. 12a**). A sample from batch three (OCLPFG-3) was used in this bio-sensing experiment. The duration of the entire bioassay, including the receptor immobilization step, lasted several hours, but the long-term stability of the system assures the absence of any long-term drift or fluctuation [**26,28**]. A limit of detection (LOD), defined as three times the standard deviation of the blank measurement (i.e. the

Published version: https://doi.org/10.1016/j.snb.2017.06.139

measurement at 0-analyte concentration), of 0.025 mg L^{-1} was achieved according to the calibration curve showed in **Fig. 12b**. Each experimental point of **Fig. 12b** is the average of 15-20 subsequent measurements taken with flow stopped at the end of each PBS washing. This value of LOD is half of that achieved in the same experimental conditions (PBS matrix and experimental setup) but using an uncoated high sensitivity TAP LPFG [**10**].

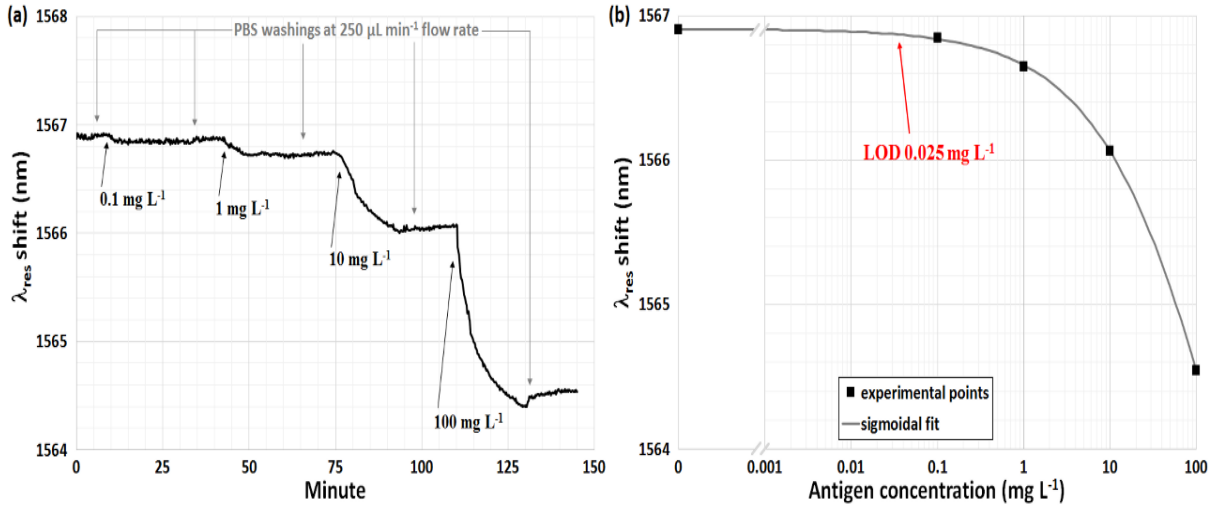

Fig. 12. Response of a sol-gel-based silica-titania coated sensor (OCLPFG-3) during the injection of the analyte when the antigen (anti-IgG) is spiked in PBS at different concentrations, 0.1, 1, 10 and 100 mg L^{-1} (**a**). The wavelength shift is monitored in real time and all the steps are highlighted with arrows (downward grey arrows during the PBS washing, black arrows during the anti-IgG binding interaction). Calibration curve of the proposed biosensor (**b**) along with the sigmoidal fitting curve (grey).

8. CONCLUSIONS

The design, fabrication and characterisation of over coupled long period fibre grating (OCLPFG) sensors and the optimization of high refractive index silica-titania sol-gel-based thin film as the overlay for those sensors have been discussed in detail. The sol-gel characteristics (composition and viscosity) and the withdrawal speed during the dip-coating deposition technique have been optimized in order to find the best combination of RI and thickness allowing the device to work in modal transition considering the PBS solution as surroundings mimicked the biological environment. Annealing temperature was optimized for the particular sol-gel material composition and for the thermal curing process to avoid the breakage of the film coating due to thermal shock. Coated OCLPFGs with overlay thickness of roughly 160 nm and RI of 1.700 were fabricated and characterised. The performance of those gratings was evaluated as both optical refractometer, in terms of volume refractive index sensitivity, and biosensor, with the implementation of a receptor-analyte (IgG/anti-IgG) bioassay. The best SRI sensitivity was roughly 7000 nm/RIU. Another OCLPFG inserted into a thermo-stabilised microfluidic system was used in the IgG/anti-IgG bioassay experiment, achieving a LOD of 0.025 mg L^{-1} in PBS matrix using a polymeric surface functionalization over the film overlay.

Published version: https://doi.org/10.1016/j.snb.2017.06.139

ACKNOWLEDGEMENTS

This research study was supported by the Joint Research Proposal (No.22/EU/Italy/CNR/proj./2012) under CSIR, India - CNR, Italy Bilateral S&T Programme, entitled “Development of Long Period Grating (LPG) based immunoassay for bio-sensing applications” and authors would like thank CSIR, INDIA for funding the Network projects ESC-110 and ESC-102. F.C. and S.T. wish to thank the European Community for the project Hemospec (FP7-611682).

References:

1. Wang, Z., Heflin, J.R., Cott, K.V., Stolen, R.H., Ramachabdran, S., Ghami, S., “Biosensor employing inonic self assembled adsorbed on long period fiber grating” Sensors and Actuators B Chemical, 139, 618-623, 2009.
2. Pilla, P., Manzillo, P.F., Malachovska, V., Buosciolo, A., Campopiano, S., Cutolo, A., Ambrosio, L., Giordano, M., Cusano, A., “Long period grating working in transition mode as promising technological platform for label-free biosensing” Optics Express, 17(2), 20039-20050, 2009.
3. Chiavaioli, F., Trono, C., Giannetti, A., Brenci, M., Baldini, F. “Characterisation of a label-free biosensor based on long period grating” Journal of Biophotonics, 7(5), 312-322, 2014.
4. Hine, A., Chen, X., Hughes, M., Zhou, K., Davies, E., Sugden, K., Bennion, I., Zhang, L., “Optical fibre-based detection of DNA hybridization” Biochemical Society Transactions, 37(2), 445-449, 2009.
5. Villar, I.D., Matías, I.R., Arregui, F.J., “Optimization of sensitivity in Long Period Fiber Gratings with overlay deposition” Optics Express, 13(1), 56-69, 2005.
6. Kim, D.W., Zhang, Y., Copper, K.L., Wang, A., “Fiber–optic interferometric immuno-sensor using long period grating” Electronics Letters, 42(6), 324-325, 2006.
7. Zhang, Y., Shibru, H., Kristie, I., Wang, A., “Miniature fiber-optic multi cavity Fabry-Perot interferometeric biosensor” Optics Letters, 30(9), 1021-1023, 2005.
8. Baldini, F., Brenci, M., Chiavaioli, F., Giannetti, A., Trono, C., “Optical fibre gratings as tools for chemical and biochemical sensing” Analytical and Bioanalytical Chemistry, 402(1), 109-116, 2012.
9. Shu, X.; Zhang, L.; Bennion, I. “Sensitivity characteristics of long-period fiber gratings” Journal of Lightwave Technology, 20(2), 255-266, 2002.
10. Chiavaioli, F., Biswas, P., Trono, C., Bandyopadhyay, S., Giannetti, A., Tombelli, S., Basumallick, N., Dasgupta, K., Baldini, F., “Towards sensitive label-free immunosensing by means of turn-around point long period fiber gratings” Biosensors and Bioelectronics, 60, 305-310, 2014.
11. Carter, R.M., Maier, R.R.J., Biswas, P., Basumallick, N., Bandyopadhyay, S., Jones, B.J.S., McCulloch, S., Barton, J.S., “Experimental Difficulties With LPG Sensors Operating Close to the Phase Turning Points” Journal of Lightwave Technology, 34(9), 3999-4004, 2016.
12. Śmietana, M., Koba, M., Mikulic, P., Bock, W.J., “Towards refractive index sensitivity of long period gratings at level of tens of μm per refractive index unit: fiber cladding etching and nano-coating deposition” Optics Express, 24(11), 11897-11904, 2016.
13. Śmietana, M., Koba, M., Mikulic, P., Bock, W.J., “Combined Plasma-Based Fiber Etching and Diamond-Like Carbon Nano Overlay Deposition for Enhancing Sensitivity of Long-Period Gratings" Journal of Lightwave Technology, 34(19), 4615-4619, 2016.
14. Karasinski, P., “Silica–Titania Films Fabricated by Sol-Gel Method for Applications in Planar Photonics” Acta Physica Polonica A, 116, 114-116, 2009.
15. Morosanova, E.I., “Silica and silica–titania sol–gel materials: Synthesis and analytical application” Talanta, 102, 114-122, 2012.

Published version: https://doi.org/10.1016/j.snb.2017.06.139

16. Ääritalo, V., Meretoja, V., Tirri, T., Areva, S., Jämsä, T., Tuukkanen, J., Rosling, A., Närhi, T., "Development of a Low Temperature Sol-Gel-Derived Titania-Silica Implant Coating" Materials Sciences and Applications, 1(3), 118-126, 2010.
17. Gu, Z., Xu, Y., "Design optimization of a long-period fiber grating with sol–gel coating for a gas sensor" Measurement Science & Technology, 18, 3530-3536, 2007.
18. Davies, E., Viitala, R., Salomäki, M., Areva, S., Zhang, L., Bennion, I., "Sol–gel derived coating applied to long-period gratings for enhanced refractive index sensing properties" Journal of Optics A: Pure and Applied Optics, 11(1), 015501, 2009.
19. Chen, H., Gu, Z., Gao, K., "Humidity sensor based on cascaded chirped long-period fiber gratings coated with TiO2/SnO2 composite films" Sensors and Actuators B Chemical, 196, 18-22, 2014.
20. Jiang, M., Li, Q.S., Wang, J.N., Jin, Z., Sui, Q., Ma, Y., Shi, J., Zhang, F., Jia, L., Yao, W.G., Dong, W.F., "TiO2 nanoparticle thin film-coated optical fiber Fabry-Perot sensor" Optics Express, 21(3), 3080-3090, 2013.
21. Beltrán-Pérez G., López-Huerta, F., Muñoz-Aguirre, S., Castillo-Mixcóatl, J., Palomino-Merino, R., Lozada-Morales, R., Portillo-Moreno, O., "Fabrication and characterization of an optical fiber pH sensor using sol–gel deposited TiO2 film doped with organic dyes" Sensors and Actuators B Chemical, 120(1), 74-78, 2006.
22. Erdogan, T., "Cladding-mode resonances in short- and long-period fiber grating filters" Journal of the Optical Societu of America A, 14(8), 1760-1773, 1997.
23. Biswas, P., Basumallick, N., Dasgupta, K., Bandyopadhyay, S., "Response of Strongly Over-Coupled Resonant Mode of a Long Period Grating to High Refractive Index Ambiance" Journal of Lightwave Technology, 32(11), 2072-2078, 2014.
24. Biswas, P., Basumallick, N., Dasgupta, K., Ghosh, A., Bandyopadhyay, S., "Application of strongly overcoupled resonant modes of long-period fiber gratings to measure the adulteration of olive oil" Applied Optics, 55(19), 5118-5126, 2016.
25. Sarkar, S., Roy, R.D., Biswas, P.K., Bhadra, S.K., Jana, S. "Mesoscale Surface Patterned Silica-Titania Sol Gel Thin Film on Glass" International Journal of Engineering and Innovative Technology, 3(10), 212-218, 2014.
26. Chiavaioli, F., Biswas, P., Trono, C., Jana, S., Bandyopadhyay, S., Basumallick, N., Giannetti, A., Tombelli, S., Bera, S., Mallick, A., Baldini, F., "Sol−Gel-Based Titania−Silica Thin Film Overlay for Long Period Fiber Grating-Based Biosensors" Analytical Chemistry, 87, 12024-12031, 2015.
27. Anemogiannis, E., Glytsis, E.N., Member, S., Gaylord, T.K., "Transmission Characteristics of Long-Period Fiber Gratings Having Arbitrary Azimuthal/Radial Refractive Index Variations" Journal Of Lightwave Technology, 21(1), 218-227, 2003.
28. Trono, C., Baldini, F., Brenci, M., Chiavaioli, F., Mugnaini, M., "Flow cell for strain-and temperature-compensated refractive index measurements by means of cascaded optical fibre long period and Bragg gratings" Measurement Science and Technology, 22, 075204, 2011.